Supporting Information for

Syntheses, structures, color tunable and white–light emitting lanthanide metal–organic framework materials constructed from conjugated 1, 1'-butadiynebenzene-3, 3', 5, 5'-tetracarboxylate ligand

Jiewei Rong,[a,b] Wenwei Zhang*[a] and Junfeng Bai*[a]

[a] *State Key Laboratory of Coordination Chemistry, School of Chemistry and Chemical Engineering, Nanjing University, Nanjing 210023, P. R. China. E–mail: wwzhang@nju.edu.cn, bjunfeng@nju.edu.cn*

[b]*School of Chemical and Materials Engineering, Huainan Normal University, Huainan, Anhui 232038, P. R. China. E–mail: zwj0076@126.com*

Details for 2–7

$[Eu_2(BBTC)_{1.5}(DMF)_4]\cdot 2DMF\cdot 4H_2O$ (2). An identical procedure with **1** was followed to prepare **2** except $SmCl_3\cdot 6H_2O$ was replaced by $EuCl_3\cdot nH_2O$. Light–yellow block–shaped crystals were achieved (yield: 70% based on Eu). Anal. calcd for $C_{48}H_{59}Eu_2N_6O_{22}$: C, 41.90; H, 4.32; N, 6.11. Found: C, 41.82; H, 4.06; N, 6.21. Selected IR data (KBr pellet, cm^{-1}): 3424 (m), 3060 (w), 2930 (w), 1648 (s), 1560 (s), 1426 (s), 1378 (s), 1113 (s), 780 (m), 714 (m).

$[Gd_2(BBTC)_{1.5}(DMF)_4]\cdot 2DMF\cdot 4H_2O$ (3). An identical procedure with **1** was followed to prepare **3** except $SmCl_3\cdot 6H_2O$ was replaced by $GdCl_3\cdot 6H_2O$. Colorless block–shaped crystals were achieved (yield: 71% based on Gd). Anal. calcd for $C_{48}H_{59}Gd_2N_6O_{22}$: C, 41.58; H, 4.29; N, 6.06. Found: C, 41.25; H, 4.19; N, 6.18 Selected IR data (KBr pellet, cm^{-1}): 3414 (m), 3062 (w), 2940 (w), 1655 (s), 1550 (s),

1418 (s), 1370 (s), 1105 (s), 787 (m), 716 (m).

$[Tb_2(BBTC)_{1.5}(DMF)_4]\cdot 2DMF\cdot 4H_2O$ (4). An identical procedure with **1** was followed to prepare **4** except $SmCl_3\cdot 6H_2O$ was replaced by $TbCl_3\cdot nH_2O$. Light–yellow block–shaped crystals were achieved (yield: 65% based on Tb). Anal. calcd for $C_{48}H_{59}Tb_2N_6O_{22}$: C, 41.48; H, 4.28; N, 6.05. Found: C, 41.35; H, 4.15; N, 6.09 Selected IR data (KBr pellet, cm^{-1}): 3374 (m), 3054 (w), 2920 (w), 1660 (s), 1550 (s), 1438 (s), 1378 (s), 1101 (s), 787 (m), 717 (m).

$[Dy_2(BBTC)_{1.5}(DMF)_4]\cdot 2DMF\cdot 4H_2O$ (5). An identical procedure with **1** was followed to prepare **5** except $SmCl_3\cdot 6H_2O$ was replaced by $DyCl_3\cdot nH_2O$. Colorless block–shaped crystals were achieved (yield: 68% based on Dy). Anal. calcd for $C_{48}H_{59}Dy_2N_6O_{22}$: C, 41.27; H, 4.26; N, 6.02. Found: C, 41.05; H, 4.18; N, 6.14. Selected IR data (KBr pellet, cm^{-1}): 3344 (m), 3036 (w), 2935 (w), 1650 (s), 1540 (s), 1420 (s), 1371 (s), 1103 (s), 778 (m), 710 (m).

$[Er_2(BBTC)_{1.5}(DMF)_4]\cdot 2DMF\cdot 4H_2O$ (6). An identical procedure with **1** was followed to prepare **6** except $SmCl_3\cdot 6H_2O$ was replaced by $ErCl_3\cdot nH_2O$. Light–pink block–shaped crystals were achieved (yield: 73% based on Er). Anal. calcd for $C_{48}H_{59}Er_2N_6O_{22}$: C, 40.99; H, 4.23; N, 5.98. Found: C, 40.64; H, 4.25; N, 6.05 Selected IR data (KBr pellet, cm^{-1}): 3390 (m), 3064 (w), 2934 (w), 1670 (s), 1560 (s), 1430 (s), 1368 (s), 1093 (s), 789 (m), 737 (m).

$[Yb_2(BBTC)_{1.5}(DMF)_4]\cdot 2DMF\cdot 4H_2O$ (7). An identical procedure with **1** was followed to prepare **7** except $SmCl_3\cdot 6H_2O$ was replaced by $YbCl_3\cdot nH_2O$. Colorless block–shaped crystals were achieved (yield: 74% based on Yb). Anal. calcd for $C_{48}H_{59}Yb_2N_6O_{22}$: C, 40.65; H, 4.19; N, 5.93. Found: C, 40.19; H, 4.14; N, 6.03 Selected IR data (KBr pellet, cm^{-1}): 3385 (m), 3042 (w), 2956 (w), 1660 (s), 1510 (s), 1460 (s), 1378 (s), 1109 (s), 789 (m), 707 (m).

Table S1 Elemental analysis and main IR bands for **1–7**

	Formula	C% (Found) [a]	H% (Found)	N% (Found)	Main IR Bands
1	$C_{48}H_{59}Sm_2N_6O_{22}$	42.00 (41.98)	4.33 (4.26)	6.12 (6.24)	3390 m, 3065 w, 2933 w, 1650 s, 1550 s, 1430 s, 1378 s, 1103 s, 787 m, 717 m
2	$C_{48}H_{59}Eu_2N_6O_{22}$	41.90 (41.82)	4.32 (4.06)	6.11 (6.21)	3424 m, 3060 w, 2930 w, 1648 s, 1560 s, 1426 s, 1378 s, 1113 s, 780 m, 714 m
3	$C_{48}H_{59}Gd_2N_6O_{22}$	41.58 (41.25)	4.29 (4.19)	6.06 (6.18)	3414 m, 3062 w, 2940 w, 1655 s, 1550 s, 1418 s, 1370 s, 1105 s, 787 m, 716 m
4	$C_{48}H_{59}Tb_2N_6O_{22}$	41.48 (41.35)	4.28 (4.15)	6.05 (6.09)	3374 m, 3054 w, 2920 w, 1660 s, 1550 s, 1438 s, 1378 s, 1101 s, 787 m, 717 m
5	$C_{48}H_{59}Dy_2N_6O_{22}$	41.27 (41.05)	4.26 (4.18)	6.02 (6.14)	3344 m, 3036 w, 2935 w, 1650 s, 1540 s, 1420 s, 1371 s, 1103 s, 778 m, 710 m
6	$C_{48}H_{59}Er_2N_6O_{22}$	40.99 (40.64)	4.23 (4.25)	5.98 (6.05)	3390 m, 3064 w, 2934 w, 1670 s, 1560 s, 1430 s, 1368 s, 1093 s, 789 m, 737 m
7	$C_{48}H_{59}Yb_2N_6O_{22}$	40.65 (40.19)	4.19 (4.14)	5.93 (6.03)	3385 m, 3042 w, 2956 w, 1660 s, 1510 s, 1460 s, 1378 s, 1109 s, 789 m, 707 m

[a]Calculated value from formula, followed by experimental value in parentheses.

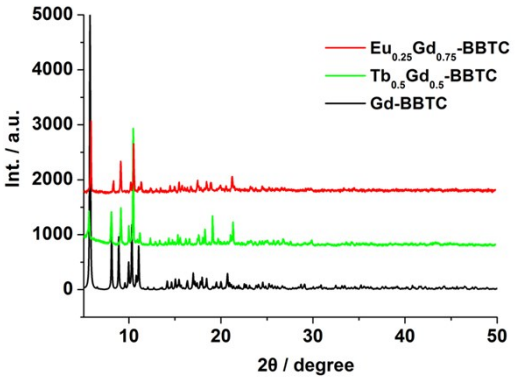

Fig. S1 Powder X−ray diffraction patterns of **Gd−BBTC**, **$Eu_{0.25}Gd_{0.75}$−BBTC** and **$Tb_{0.5}Gd_{0.5}$−BBTC** at ambient temperature.

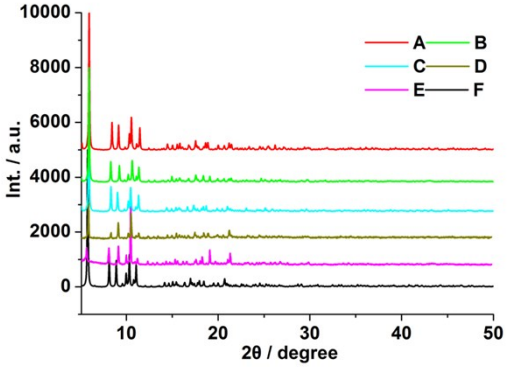

Fig. S2 The PXRD patterns for complex **Gd−BBTC** (**F**) and the co−doped complexes $\mathbf{Eu_xTb_yGd_{1-x-y}}$**−BBTC** (**A−E)** (Eu, Tb, Gd%): **A** (4.5, 5.5, 90), **B** (4, 5, 91), **C** (3, 4.5, 92.5), **D** (2.5, 4, 93.5) and **E** (1.5, 3.5, 95).

Table S2 Elemental analysis for $\mathbf{Eu_xGd_{1-x}}$**−BBTC** and $\mathbf{Tb_yGd_{1-y}}$**−BBTC** co−doped compounds

Ln−BBTC	Wt% C	Wt% H	Wt% N
	Calcd (Found)	Calcd (Found)	Calcd (Found)
$\mathbf{Eu_{0.40}Gd_{0.60}}$**−BBTC**	41.72 (41.59)	4.30 (4.09)	6.08 (6.09)
$\mathbf{Eu_{0.25}Gd_{0.75}}$**−BBTC**	41.66 (41.37)	4.30 (4.25)	6.07 (6.19)
$\mathbf{Tb_{0.75}Gd_{0.25}}$**−BBTC**	41.50 (41.24)	4.28 (4.05)	6.05 (6.12)
$\mathbf{Tb_{0.50}Gd_{0.50}}$**−BBTC**	41.53 (41.35)	4.28 (4.03)	6.05 (6.18)
$\mathbf{Tb_{0.25}Gd_{0.75}}$**−BBTC**	41.56 (41.43)	4.29 (4.15)	6.06 (6.14)

Table S3 Elemental analysis for $\mathbf{Eu_xTb_yGd_{1-x-y}}$**−BBTC** co−doped compounds

Ln−BBTC	Wt% C	Wt% H	Wt% N
	Calcd (Found)	Calcd (Found)	Calcd (Found)
$\mathbf{Eu_{0.045}Tb_{0.055}Gd_{0.9}}$**−BBTC**	41.59 (41.26)	4.29 (4.18)	6.06 (6.12)
$\mathbf{Eu_{0.04}Tb_{0.05}Gd_{0.91}}$**−BBTC**	41.58 (41.34)	4.29 (4.15)	6.06 (6.15)
$\mathbf{Eu_{0.03}Tb_{0.045}Gd_{0.925}}$**−BBTC**	41.58 (41.41)	4.29 (4.21)	6.06 (5.95)
$\mathbf{Eu_{0.025}Tb_{0.04}Gd_{0.935}}$**−BBTC**	41.58 (41.39)	4.29 (4.13)	6.06 (6.09)
$\mathbf{Eu_{0.015}Tb_{0.035}Gd_{0.95}}$**−BBTC**	41.58 (41.29)	4.29 (4.18)	6.06 (6.01)

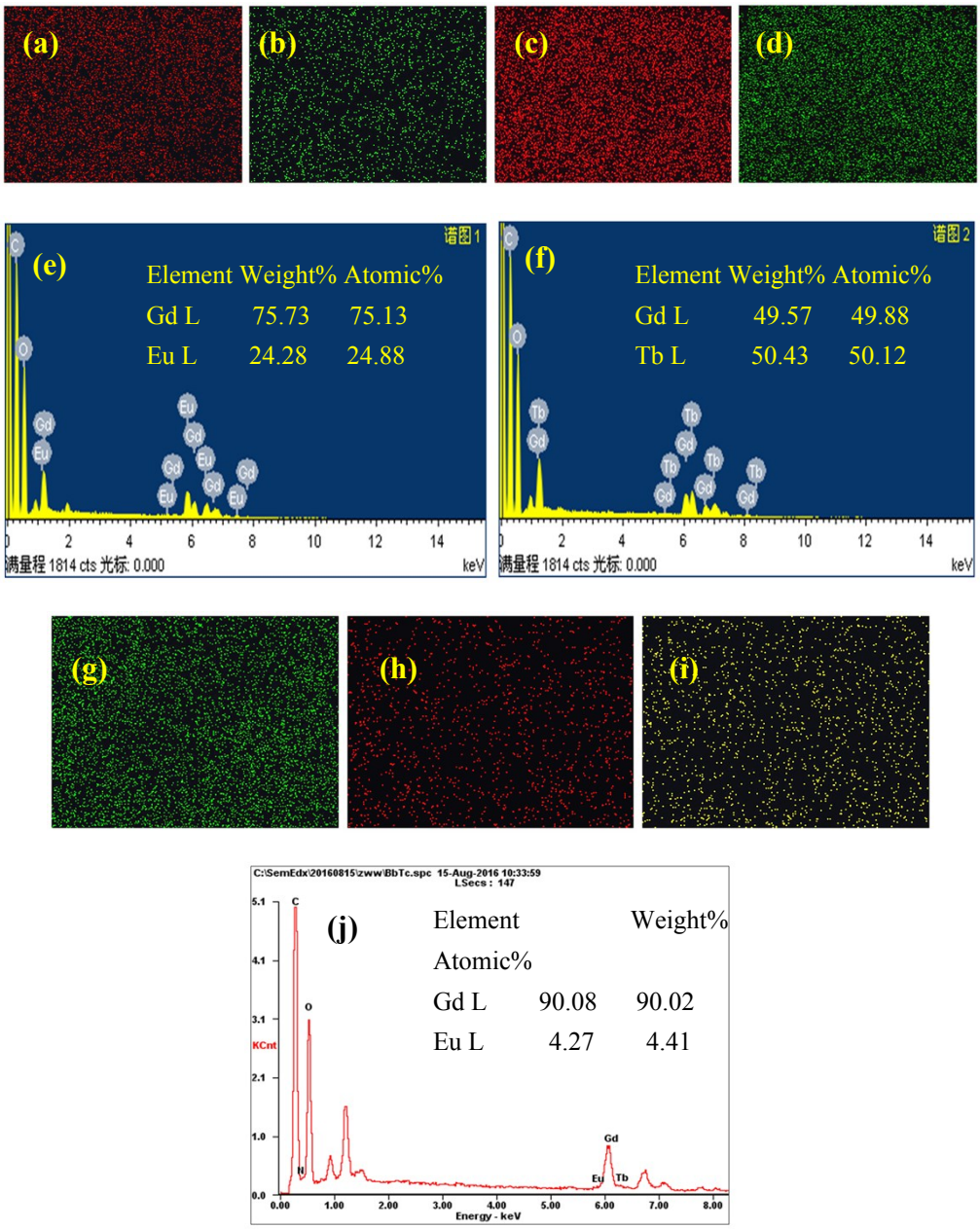

Fig. S3 Elemental mapping images of (a, b) **$Eu_{0.25}Gd_{0.75}$−BBTC** (red and green dots represent the Gd and the Eu elements, respectively), (c, d) **$Tb_{0.50}Gd_{0.50}$−BBTC** (red and green dots represent the Gd and the Tb elements, respectively) and (g, h, i) **$Eu_{0.045}Tb_{0.055}Gd_{0.9}$−BBTC** (green, red and yellow dots represent the Gd, Eu and Tb elements, respectively), and EDX−spectra of (e) **$Eu_{0.25}Gd_{0.75}$−BBTC**, (f) **$Tb_{0.50}Gd_{0.50}$−BBTC** and (j) **$Eu_{0.045}Tb_{0.055}Gd_{0.9}$−BBTC**.

Table S4 ICP analysis for $\mathbf{Eu_xGd_{1-x}}$**−BBTC**, $\mathbf{Tb_yGd_{1-y}}$**−BBTC** and $\mathbf{Eu_xTb_yGd_{1-x-y}}$**−BBTC** co−doped compounds

Ln−BBTC	Wt% Gd Calcd (Found)	Wt% Eu Calcd (Found)	Wt% Tb Calcd (Found)
$\mathbf{Eu_{0.25}Gd_{0.75}}$**−BBTC**	75.64 (75.42)	24.36 (24.58)	–
$\mathbf{Tb_{0.5}Gd_{0.5}}$**−BBTC**	49.74 (49.50)	–	50.26 (50.50)
$\mathbf{Eu_{0.045}Tb_{0.055}Gd_{0.9}}$**−BBTC**	90.09 (89.85)	4.35 (4.52)	5.56 (5.63)

Table S5 Crystallographic data and structural refinements for **1** and **3**

Compound	**1**	**3**
Formula	$C_{48}H_{59}Sm_2N_6O_{22}$	$C_{48}H_{59}Gd_2N_6O_{22}$
Formula weight	1373	1387
Temperature (K)	296(2)	296(2)
Crystal system	monoclinic	monoclinic
Space group	*C*2/*c*	*C*2/*c*
a (Å)	29.919(5)	30.62(4)
b (Å)	21.281(3)	21.76(3)
c (Å)	19.185(3)	19.90(3)
α (deg)	90.00	90.00
β (deg)	93.690(4)	93.52(2)
γ (deg)	90.00	90.00
V (Å^3)	12190(3)	13231(31)
Z	8	8
F(000)	4552	4584
GOF	1.079	1.021
R_1, wR_2 [$I > 2\sigma(I)$] [a]	0.1225, 0.2493	0.0885, 0.2018

[a] $R_1 = \Sigma||F_o|-|F_c||/\Sigma|F_o|$; w$R_2 = \{\Sigma\,[w(F_o^2-F_c^2)^2]/\Sigma(w(F_o^2)^2]\}^{1/2}$

Table S6 Selected bond distances (Å) in **1–7**

			1		
Sm1–O11	2.332(5)	Sm1–O13	2.372(7)	Sm1–O6	2.373(5)
Sm1–O5	2.402(5)	Sm1–O12	2.417(5)	Sm1–O15	2.438(6)
Sm1–O2	2.455(5)	Sm1–O1	2.477(5)	Sm2–O16	2.287(7)
Sm2–O3	2.319(5)	Sm2–O4	2.337(5)	Sm2–O9	2.388(6)
Sm2–O14	2.426(7)	Sm2–O8	2.429(5)	Sm2–O10	2.507(6)
Sm2–O7	2.508(5)				
			2		
Eu1–O11	2.332(3)	Eu1–O6	2.364(3)	Eu1–O5	2.390(3)
Eu1–O12	2.406(3)	Eu1–O13	2.419(5)	Eu1–O14	2.419(5)
Eu1–O2	2.444(3)	Eu1–O1	2.496(3)	Eu2–O4	2.297(3)
Eu2–O3	2.303(4)	Eu2–O15	2.343(6)	Eu2–O16	2.377(8)
Eu2–O10	2.415(4)	Eu2–O8	2.418(3)	Eu2–O9	2.488(4)
Eu2–O7	2.489(3)				
			3		
Gd1–O8	2.368(10)	Gd1–O11	2.374(9)	Gd1–O15	2.401(16)
Gd1–O7	2.419(12)	Gd1–O16	2.448(14)	Gd1–O12	2.465(9)
Gd1–O2	2.492(10)	Gd1–O1	2.536(10)	Gd2–O13	2.186(17)
Gd2–O3	2.331(11)	Gd2–O4	2.350(10)	Gd2–O14	2.402(16)
Gd2–O6	2.453(12)	Gd2–O9	2.463(11)	Gd2–O10	2.537(11)
Gd2–O5	2.544(8)				
			4		
Tb1–O11	2.299(4)	Tb1–O8	2.327(4)	Tb1–O7	2.362(5)
Tb1–O12	2.370(4)	Tb1–O17	2.399(7)	Tb1–O19	2.400(14)
Tb1–O1	2.421(4)	Tb1–O2	2.464(4)	Tb2–O4	2.277(5)
Tb2–O3	2.287(5)	Tb2–O18	2.316(8)	Tb2–O20	2.324(7)
Tb2–O9	2.368(18)	Tb2–O6	2.402(5)	Tb2–O10	2.44(2)
Tb2–O5	2.471(4)				
			5		
Dy1–O11	2.294(6)	Dy1–O8	2.324(5)	Dy1–O7	2.353(6)
Dy1–O12	2.370(5)	Dy1–O2	2.389(6)	Dy1–O16	2.395(8)
Dy1–O13	2.395(9)	Dy1–O1	2.458(6)	Dy2–O4	2.274(5)
Dy2–O3	2.284(7)	Dy2–O14	2.285(11)	Dy2–O15	2.319(11)
Dy2–O9	2.365(7)	Dy2–O6	2.396(6)	Dy2–O10	2.447(7)
Dy2–O5	2.454(5)				
			6		
Er1–O11	2.265(6)	Er1–O8	2.276(5)	Er1–O7	2.335(6)
Er1–O12	2.345(6)	Er1–O1	2.356(7)	Er1–O13	2.374(9)
Er1–O14	2.393(9)	Er1–O2	2.427(6)	Er2–O4	2.256(5)
Er2–O3	2.287(7)	Er2–O16	2.292(10)	Er2–O15	2.300(11)
Er2–O9	2.356(7)	Er2–O6	2.380(6)	Er2–O10	2.421(7)
Er2–O5	2.435(5)				

			7		
Yb1–O11	2.248(6)	Yb1–O8	2.260(5)	Yb1–O7	2.300(6)
Yb1–O12	2.303(5)	Yb1–O2	2.319(6)	Yb1–O13	2.321(9)
Yb1–O1	2.397(6)	Yb1–O14	2.405(9)	Yb2–O4	2.216(6)
Yb2–O3	2.242(7)	Yb2–O15	2.265(10)	Yb2–O16	2.281(11)
Yb2–O10	2.324(7)	Yb2–O6	2.349(6)	Yb2–O9	2.412(7)
Yb2–O5	2.423(5)				

Table S7 Selected bond angles (°) in **1–7**

		1	
O11–Sm1–O13	142.5(2)	O11–Sm1–O6	76.72(18)
O13–Sm1–O6	75.61(19)	O11–Sm1–O5	78.77(18)
O13–Sm1–O5	138.61(19)	O6–Sm1–O5	126.89(16)
O11–Sm1–O12	123.37(18)	O13–Sm1–O12	75.4(2)
O6–Sm1–O12	79.59(17)	O5–Sm1–O12	75.93(18)
O11–Sm1–O15	81.5(2)	O13–Sm1–O15	66.6(2)
O6–Sm1–O15	73.30(18)	O5–Sm1–O15	146.50(19)
O12–Sm1–O15	137.5(2)	O11–Sm1–O2	85.96(18)
O13–Sm1–O2	103.2(2)	O6–Sm1–O2	145.47(17)
O5–Sm1–O2	77.05(18)	O12–Sm1–O2	134.24(18)
O15– Sm1–O2	74.8(2)	O11–Sm1–O1	136.00(19)
O13–Sm1–O1	70.5(2)	O6–Sm1–O1	145.56(18)
O5–Sm1–O1	78.55(18)	O12–Sm1–O1	86.34(17)
O15–Sm1–O1	97.87(19)	O2–Sm1–O1	52.37(17)
O16–Sm2–O3	85.5(2)	O16–Sm2–O4	151.5(2)
O3–Sm2–O4	90.16(18)	O16– Sm2–O9	86.1(2)
O3–Sm2–O9	150.58(19)	O4–Sm2–O9	110.0(2)
O16–Sm2–O14	71.1(2)	O3–Sm2–O14	81.7(2)
O4–Sm2–O14	80.5(2)	O9–Sm2–O14	121.7(2)
O16–Sm2–O8	129.7(2)	O3–Sm2–O8	84.77(19)
O4–Sm2–O8	77.63(18)	O9–Sm2–O8	79.16(19)
O14–Sm2–O8	154.15(18)	O16–Sm2–O10	94.7(2)
O3–Sm2–O10	158.06(19)	O4–Sm2–O10	79.24(18)
O9–Sm2–O10	50.91(19)	O14–Sm2–O10	77.6(2)
O8–Sm2–O10	111.19(19)	O16–Sm2–O7	77.2(2)
O3–Sm2–O7	77.21(17)	O4–Sm2–O7	129.16(19)
O9–Sm2–O7	73.44(18)	O14–Sm2–O7	142.97(19)
O8–Sm2–O7	52.55(16)	O10–Sm2–O7	124.28(17)
		2	
O11–Eu1–O6	77.33(11)	O11–Eu1–O5	78.00(12)
O6–Eu1–O5	127.15(10)	O11–Eu1–O12	124.34(11)
O6–Eu1–O12	79.78(11)	O5–Eu1–O12	76.94(12)

O11–Eu1–O13	142.59(16)	O6–Eu1–O13	74.67(14)
O5–Eu1–O13	139.23(15)	O12–Eu1–O13	74.11(16)
O11–Eu1–O14	77.60(15)	O6–Eu1–O14	75.49(15)
O5–Eu1–O14	141.07(15)	O12–Eu1–O14	141.95(16)
O13–Eu1–O14	71.75(18)	O11–Eu1–O2	85.63(10)
O6–Eu1–O2	144.08(12)	O5–Eu1–O2	78.29(12)
O12–Eu1–O2	135.01(11)	O13–Eu1–O2	103.09(15)
O14–Eu1–O2	70.03(15)	O11–Eu1–O1	135.21(11)
O6–Eu1–O1	145.90(11)	O5–Eu1–O1	78.07(11)
O12–Eu1–O1	85.65(10)	O13–Eu1–O1	71.73(15)
O14–Eu1–O1	99.02(14)	O2–Eu1–O1	52.66(9)
O4–Eu2–O3	87.43(12)	O4–Eu2–O15	79.94(17)
O3–Eu2–O15	78.19(19)	O4–Eu2–O16	87.45(18)
O3–Eu2–O16	150.0(2)	O15–Eu2–O16	71.8(2)
O4–Eu2–O10	153.10(13)	O3–Eu2–O10	111.97(15)
O15–Eu2–O10	121.05(18)	O16–Eu2–O10	84.2(2)
O4–Eu2–O8	86.00(14)	O3–Eu2–O8	80.11(12)
O15–Eu2–O8	154.56(17)	O16–Eu2–O8	128.96(19)
O10–Eu2–O8	79.57(16)	O4–Eu2–O9	154.89(12)
O3–Eu2–O9	78.61(12)	O15–Eu2–O9	76.85(18)
O16–Eu2–O9	94.24(18)	O10–Eu2–O9	51.63(13)
O8–Eu2–O9	111.60(15)	O4–Eu2–O7	79.33(11)
O3–Eu2–O7	131.57(12)	O15–Eu2–O7	142.31(18)
O16–Eu2–O7	76.18(18)	O10–Eu2–O7	73.85(12)
O8–Eu2–O7	52.86(10)	O9–Eu2–O7	125.42(11)
		3	
O8–Gd1–O11	77.7(4)	O8–Gd1–O15	77.1(4)
O11–Gd1–O15	76.4(4)	O8–Gd1–O7	126.3(3)
O11–Gd1–O7	77.6(4)	O15–Gd1–O7	139.4(4)
O8–Gd1–O16	76.4(4)	O11–Gd1–O16	144.0(5)
O15–Gd1–O16	73.8(5)	O7–Gd1–O16	138.4(4)
O8–Gd1–O12	79.8(4)	O11–Gd1–O12	124.2(3)
O15–Gd1–O12	144.4(5)	O7–Gd1–O12	76.2(4)
O16–Gd1–O12	74.8(4)	O8–Gd1–O2	145.1(4)
O11–Gd1–O2	85.2(3)	O15–Gd1–O2	69.4(5)
O7–Gd1–O2	77.8(4)	O16–Gd1–O2	102.4(4)
O12–Gd1–O2	134.3(4)	O8–Gd1–O1	145.8(4)
O11–Gd1–O1	135.0(4)	O15–Gd1–O1	98.8(4)
O7–Gd1–O1	78.7(4)	O16–Gd1–O1	70.0(4)
O12–Gd1–O1	85.6(3)	O2–Gd1–O1	52.6(3)
O13–Gd2–O3	146.8(5)	O13–Gd2–O4	92.0(5)
O3–Gd2–O4	88.3(4)	O13–Gd2–O14	70.2(5)
O3–Gd2–O14	77.2(5)	O4–Gd2–O14	80.6(4)
O13–Gd2–O6	131.4(4)	O3–Gd2–O6	81.7(4)

O4–Gd2–O6	86.0(4)	O14–Gd2–O6	155.2(4)
O13–Gd2–O9	79.0(5)	O3–Gd2–O9	113.5(4)
O4–Gd2–O9	152.3(3)	O14–Gd2–O9	119.5(4)
O6–Gd2–O9	80.8(4)	O13–Gd2–O10	87.9(5)
O3–Gd2–O10	78.6(4)	O4–Gd2–O10	155.2(4)
O14–Gd2–O10	76.1(4)	O6–Gd2–O10	112.4(4)
O9–Gd2–O10	51.5(3)	O13–Gd2–O5	79.0(5)
O3–Gd2–O5	133.3(4)	O4–Gd2–O5	79.5(3)
O14–Gd2–O5	142.4(4)	O6–Gd2–O5	52.8(3)
O9–Gd2–O5	73.1(3)	O10–Gd2–O5	124.6(3)
		4	
O11–Tb1–O8	77.48(16)	O11–Tb1–O7	78.20(17)
O8–Tb1–O7	126.98(16)	O11–Tb1–O12	124.21(17)
O8–Tb1–O12	79.42(17)	O7–Tb1–O12	76.69(17)
O11–Tb1–O17	142.5(2)	O8–Tb1–O17	75.19(19)
O7–Tb1–O17	139.2(2)	O12–Tb1–O17	74.9(2)
O11–Tb1–O19A	83.2(6)	O8–Tb1–O19A	74.5(7)
O7–Tb1–O19A	146.4(6)	O12–Tb1–O19A	136.5(6)
O17–Tb1–O19A	65.2(6)	O11–Tb1–O19	74.5(5)
O8–Tb1–O19	76.6(5)	O7–Tb1–O19	138.3(5)
O12–Tb1–O19	145.0(5)	O17–Tb–O19	74.6(5)
O9–Tb2–O10A	48.6(7)	O11–Tb1–O1	84.85(16)
O8–Tb1–O1	144.11(18)	O7–Tb1–O1	78.12(19)
O12–Tb1–O1	135.56(17)	O17–Tb1–O1	103.0(2)
O19A –Tb1–O1	72.5(6)	O19–Tb1–O1	68.6(5)
O11–Tb1–O2	135.15(16)	O8–Tb1–O2	145.72(15)
O7–Tb1–O2	78.35(16)	O12–Tb1–O2	86.13(15)
O17–Tb1–O2	71.1(2)	O19A–Tb1–O2	96.2(6)
O19–Tb1–O2	99.7(5)	O1–Tb1–O2	53.12(14)
O4–Tb2–O3	87.84(19)	O4–Tb2–O18A	78.6(5)
O3–Tb2–O18A	146.6(5)	O4–Tb2–O18	93.0(4)
O3–Tb2–O18	151.1(4)	O6–Tb2–O10A	104.4(12)
O4–Tb2–O20	80.4(2)	O3–Tb2–O20	77.8(3)
O18A–Tb2–O20	70.0(6)	O18–Tb2–O20	73.9(5)
O4–Tb2–O9	154.1(4)	O3–Tb2–O9	105.9(8)
O18A–Tb2–O9	99.1(9)	O18–Tb2–O9	85.3(9)
O20–Tb2–O9	123.5(4)	O4–Tb2–O6	86.0(2)
O3–Tb2–O6	79.96(18)	O18A–Tb2–O6	128.5(6)
O18–Tb2–O6	128.9(4)	O20–Tb2–O6	154.3(3)
O9–Tb2–O6	75.2(5)	O4–Tb2–O10	153.3(3)
O3–Tb2–O10	81.7(6)	O18A–Tb2–O10	96.9(9)
O18–Tb2–O10	84.8(8)	O20–Tb2–O10	73.5(5)
O9–Tb2–O10	52.4(3)	O6–Tb2–O10	115.8(6)
O4–Tb2–O9A	149.5(5)	O3–Tb2–O9A	120.6(10)

O18A–Tb2–O9A	81.6(14)	O18–Tb2–O9A	67.6(15)
O20–Tb2–O9A	114.0(12)	O5–Tb2–O10A	123.5(7)
O6–Tb2–O9A	88.5(14)	O10–Tb2–O9A	52.1(5)
O4–Tb2–O5	79.55(16)	O3–Tb2–O5	131.95(17)
O18A–Tb2–O5	75.6(6)	O18–Tb2–O5	76.3(4)
O20–Tb2–O5	142.9(3)	O9–Tb2–O5	74.9(5)
O6–Tb2–O5	53.24(15)	O10–Tb2–O5	125.2(3)
O9A–Tb2–O5	73.2(5)	O4–Tb2–O10A	156.6(6)
O3–Tb2–O10A	73.8(6)	O18A–Tb2–O10A	108.9(11)
O18–Tb2–O10A	96.2(10)	O20–Tb2–O10A	81.6(11)
		5	
O11–Dy1–O8	77.2(2)	O11–Dy1–O7	78.6(2)
O8–Dy1–O7	126.72(18)	O11–Dy1–O12	125.1(2)
O8–Dy1–O12	79.6(2)	O7–Dy1–O12	76.8(2)
O11–Dy1–O2	84.4(2)	O8–Dy1–O2	143.5(2)
O7–Dy1–O2	78.8(2)	O12–Dy1–O2	135.9(2)
O11–Dy1–O16	78.2(3)	O8–Dy1–O16	74.4(2)
O7–Dy1–O16	143.4(2)	O12–Dy1–O16	139.8(3)
O2–Dy1–O16	71.1(3)	O11–Dy1–O13	142.4(3)
O8–Dy1–O13	75.0(2)	O7–Dy1–O13	138.8(3)
O12–Dy1–O13	73.7(3)	O2–Dy1–O13	103.6(2)
O16–Dy1–O13	70.3(3)	O11–Dy1–O1	134.9(2)
O8–Dy1–O1	146.0(2)	O7–Dy1–O1	78.7(2)
O12–Dy1–O1	86.3(2)	O2–Dy1–O1	53.1(2)
O16–Dy1–O1	98.5(2)	O13–Dy1–O1	71.3(3)
O4–Dy2–O3	88.2(2)	O4–Dy2–O14	78.6(3)
O3–Dy2–O14	77.7(3)	O4–Dy2–O15	88.4(3)
O3–Dy2–O15	149.5(3)	O14–Dy2–O15	71.9(4)
O4–Dy2–O9	152.6(2)	O3–Dy2–O9	111.3(3)
O14–Dy2–O9	123.2(3)	O15–Dy2–O9	83.9(3)
O4–Dy2–O6	85.4(2)	O3–Dy2–O6	80.1(2)
O14–Dy2–O6	152.9(3)	O15–Dy2–O6	129.8(3)
O9–Dy2–O6	79.6(3)	O4–Dy2–O10	154.6(2)
O3–Dy2–O10	78.1(2)	O14–Dy2–O10	77.7(3)
O15–Dy2–O10	92.7(3)	O9–Dy2–O10	52.4(2)
O6–Dy2–O10	112.6(2)	O4–Dy2–O5	79.8(2)
O3–Dy2–O5	132.5(2)	O14–Dy2–O5	141.8(3)
O15–Dy2–O5	76.4(3)	O9–Dy2–O5	72.9(2)
O6–Dy2–O5	53.43(18)	O10–Dy2–O5	125.1(2)
		6	
O11–Er1–O8	77.3(2)	O11–Er1–O7	78.4(2)
O8–Er1–O7	127.21(19)	O11–Er1–O12	125.4(2)
O8–Er1–O12	80.2(2)	O7–Er1–O12	77.1(2)
O11–Er1–O1	84.4(2)	O8–Er1–O1	141.4(2)

O7–Er1–O1	80.5(2)	O12–Er1–O1	136.9(2)
O11–Er1–O13	141.5(3)	O8–Er1–O13	74.7(2)
O7–Er1–O13	140.0(3)	O12–Er1–O13	74.8(3)
O1–Er1–O13	101.6(3)	O11–Er1–O14	78.6(3)
O8–Er1–O14	72.1(3)	O7–Er1–O14	144.9(2)
O12–Er1–O14	138.1(3)	O1–Er1–O14	71.2(3)
O13–Er1–O14	68.0(3)	O11–Er1–O2	134.5(2)
O8–Er1–O2	146.1(2)	O7–Er1–O2	78.6(2)
O12–Er1–O2	86.2(2)	O1–Er1–O2	53.3(2)
O13–Er1–O2	71.8(3)	O14–Er1–O2	99.6(3)
O4–Er2–O3	88.9(2)	O4–Er2–O16	79.2(3)
O3–Er2–O16	77.0(3)	O4–Er2–O15	90.1(3)
O3–Er2–O15	149.9(3)	O16–Er2–O15	73.3(3)
O4–Er2–O9	152.2(2)	O3–Er2–O9	110.6(3)
O16– Er2– O9	123.4(3)	O15–Er2–O9	82.6(3)
O4–Er2–O6	85.2(2)	O3–Er2–O6	79.0(2)
O16–Er2–O6	151.5(3)	O15–Er2–O6	130.9(3)
O9–Er2–O6	79.7(3)	O4–Er2–O10	154.4(2)
O3–Er2–O10	78.7(2)	O16–Er2–O10	76.3(3)
O15–Er2–O10	89.7(3)	O9–Er2–O10	52.8(2)
O6–Er2–O10	113.7(2)	O4–Er2–O5	79.62(19)
O3–Er2–O5	132.2(2)	O16–Er2–O5	143.2(3)
O15–Er2–O5	77.0(3)	O9–Er2–O5	72.6(2)
O6–Er2–O5	54.02(19)	O10–Er2–O5	125.1(2)
		7	
O11–Yb1–O8	77.1(2)	O11–Yb1–O7	78.9(2)
O8–Yb1–O7	128.07(19)	O11–Yb1–O12	125.5(2)
O8–Yb1–O12	79.4(2)	O7–Yb1–O12	78.4(2)
O11–Yb1–O2	83.9(2)	O8–Yb1–O2	139.2(2)
O7–Yb1–O2	81.7(2)	O12–Yb1–O2	139.5(2)
O11–Yb1–O13	138.8(3)	O8–Yb1–O13	74.8(2)
O7–Yb1–O13	142.2(3)	O12–Yb1–O13	77.6(3)
O2–Yb1–O13	98.4(3)	O11–Yb1–O1	134.9(2)
O8–Yb1–O1	145.7(2)	O7–Yb1–O1	78.2(2)
O12 –Yb–O1	86.6(2)	O2–Yb1–O1	54.8(2)
O13–Yb1–O1	71.7(3)	O11–Yb1–O14	77.5(3)
O8–Yb1–O14	73.3(3)	O7–Yb1–O14	142.7(3)
O12–Yb1–O14	138.8(3)	O2–Yb1–O14	67.5(3)
O13–Yb1–O14	66.0(3)	O1–Yb1–O14	99.0(2)
O4–Yb2–O3	88.8(2)	O4–Yb2–O15	79.4(3)
O3–Yb2–O15	77.4(3)	O4–Yb2–O16	88.8(3)
O3–Yb2–O16	149.4(3)	O15–Yb2–O16	72.1(4)
O4–Yb2–O10	152.6(2)	O3–Yb2–O10	109.3(3)
O15–Yb2–O10	123.7(3)	O16–Yb2–O10	85.5(3)

O4–Yb2– O6	85.3(2)	O3–Yb2–O6	79.0(2)
O15–Yb2– O6	152.0(3)	O16–Yb2–O6	131.2(3)
O10–Yb2–O6	78.5(3)	O4– Yb2– O9	154.4(2)
O3–Yb2–O9	78.1(2)	O15–Yb2–O9	76.3(3)
O16–Yb2–O9	91.5(3)	O10–Yb2–O9	52.8(2)
O6–Yb2–O9	113.1(2)	O4–Yb2–O5	79.6(2)
O3–Yb2–O5	132.2(2)	O15–Yb2–O5	142.9(3)
O16–Yb2–O5	77.2(3)	O10–Yb2–O5	73.0(2)
O6–Yb2–O5	54.09(19)	O9–Yb2–O5	125.4(2)

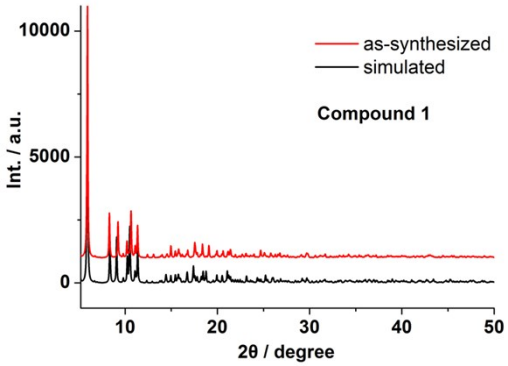

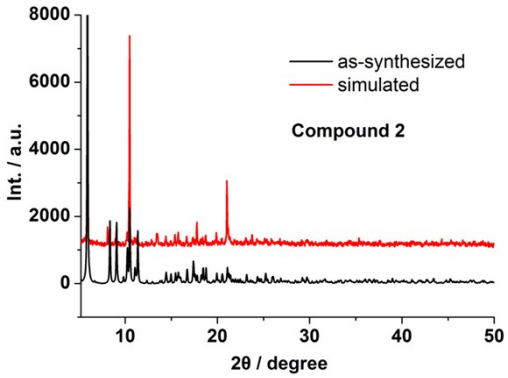

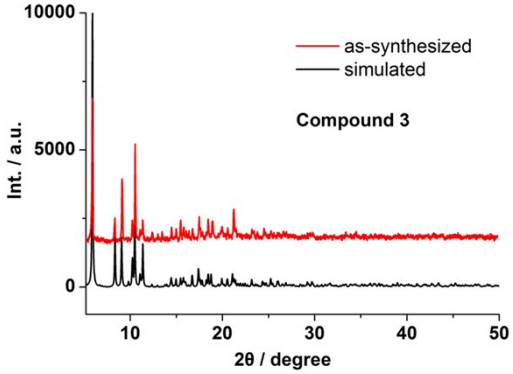
10000
5000
0
Int. / a.u.
10
20
30
40
50
2θ / degree
as-synthesized
simulated
Compound 3

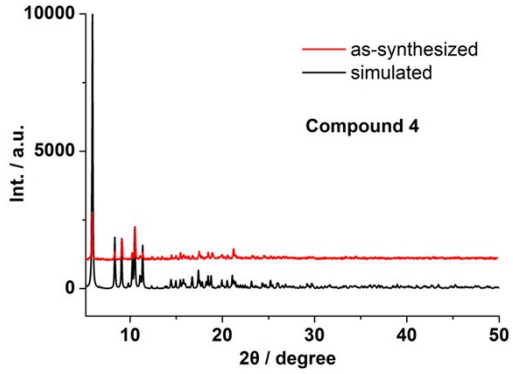
10000
5000
0
Int. / a.u.
10
20
30
40
50
2θ / degree
as-synthesized
simulated
Compound 4

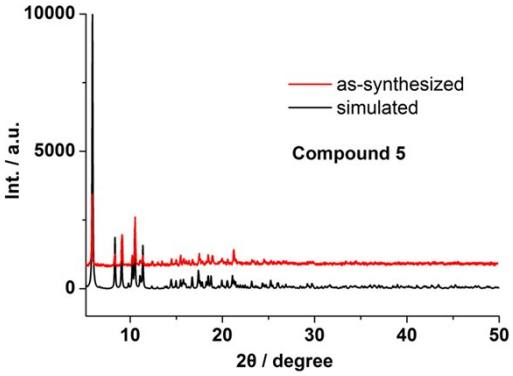
10000
5000
0
Int. / a.u.
10
20
30
40
50
2θ / degree
as-synthesized
simulated
Compound 5

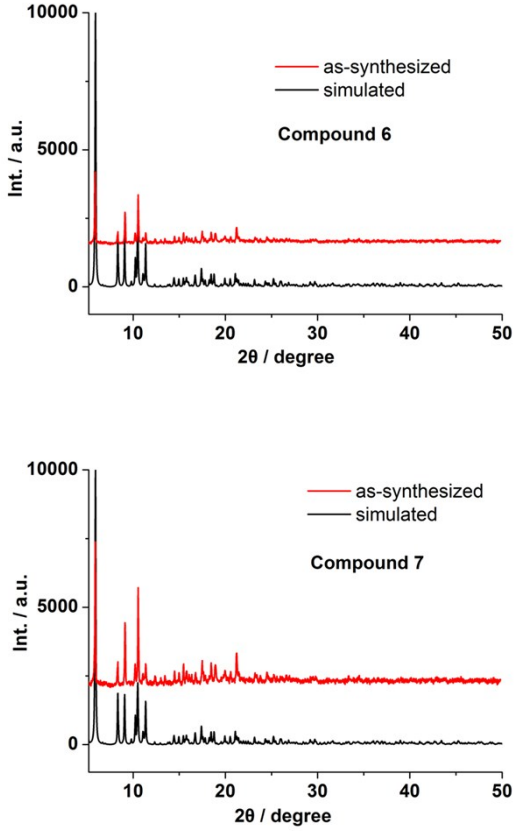

Fig. S4 PXRD patterns of simulated from the X–ray single–crystal structures and as–synthesized samples of **1–7**.

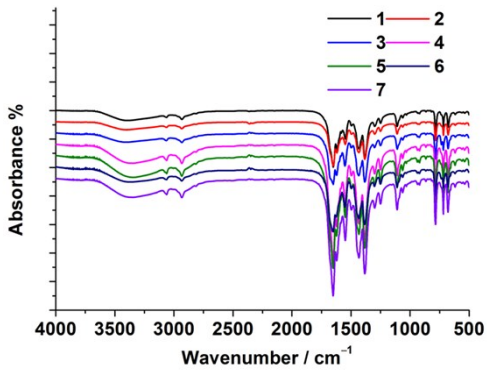

Fig. S5 The IR spectra of **1–7** recorded from a KBr pellet.

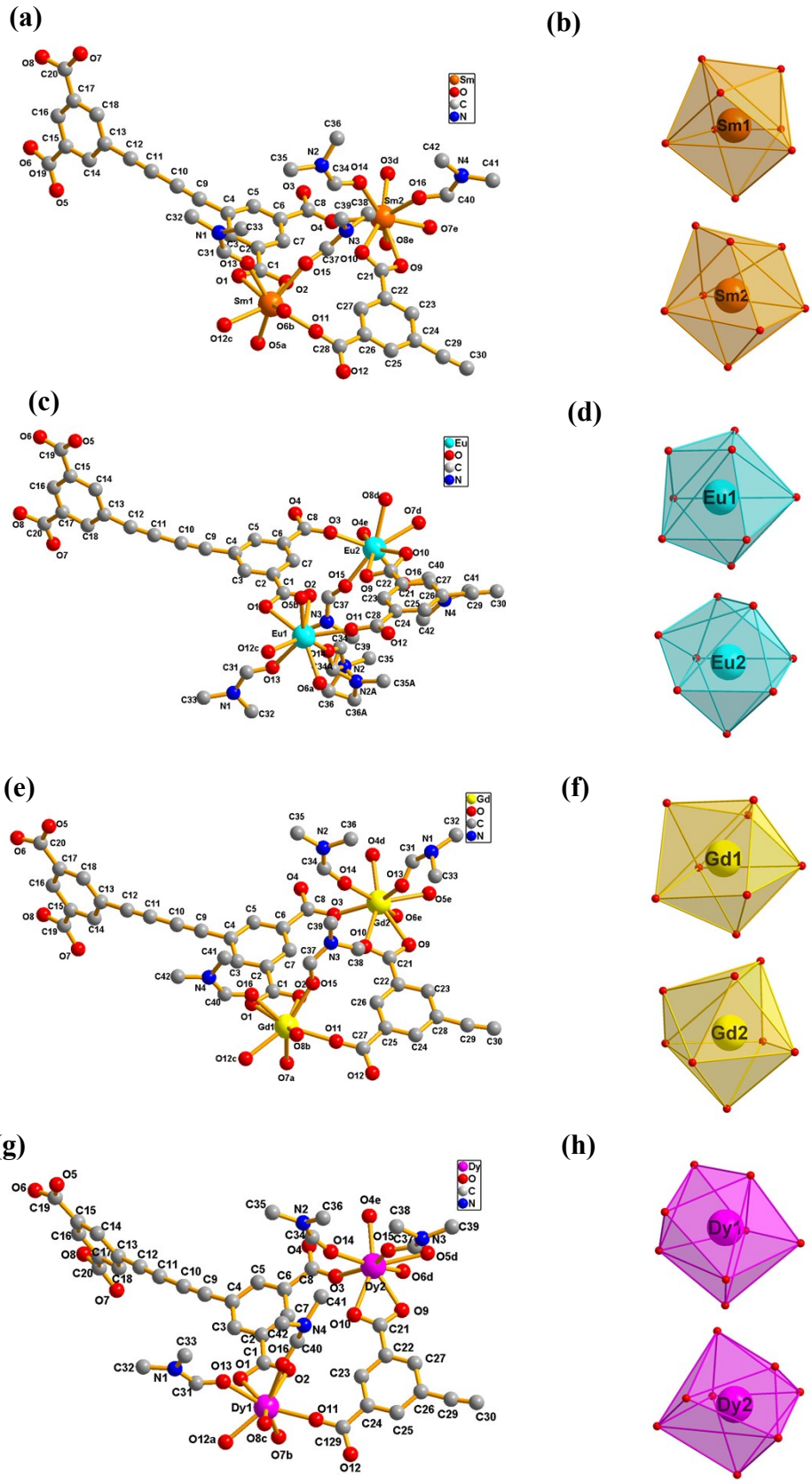
(a)
(b)
(c)
(d)
(e)
(f)
(g)
(h)
Sm
O
C
N
Sm1
Sm2
Eu
Eu1
Eu2
Gd
Gd1
Gd2
Dy
Dy1
Dy2

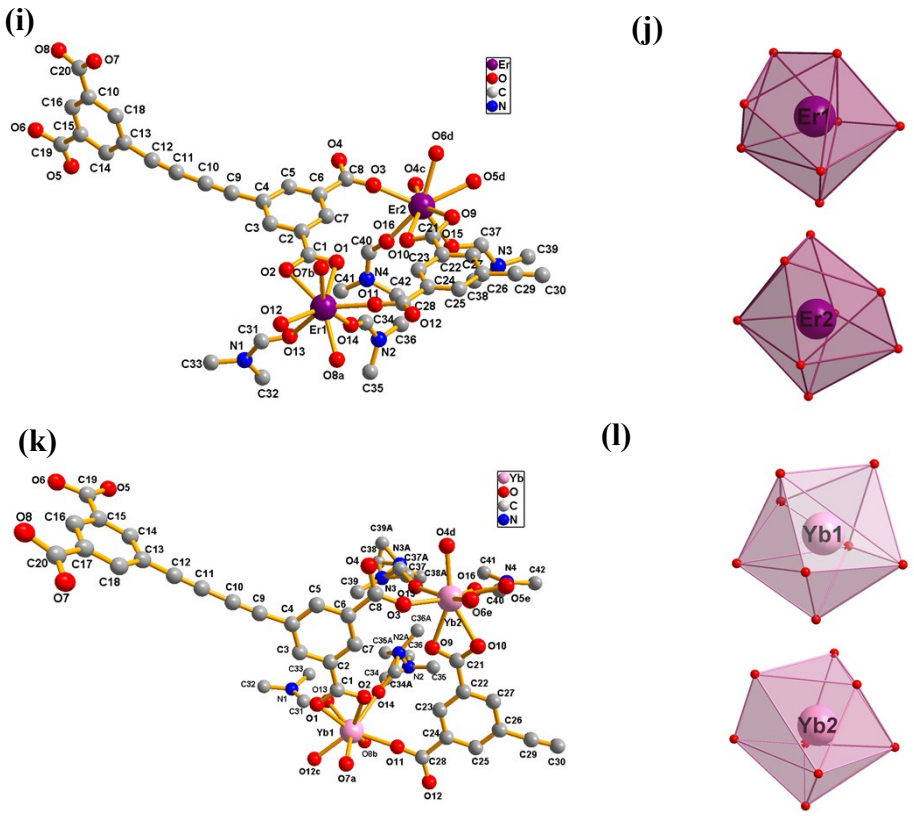

Fig. S6 (a) Coordination environments of Sm^{3+} ions with the H atoms omitted for clarity; symmetry codes: a = 0.5–x, 1.5+y, 0.5–z; b = 1+x, 2–y, 0.5+z; c = 1–x, 2+y, 0.5–z; d = 1–x, 1+y, 0.5–z; e = 1+x, 1+y, 1+z; (b) Coordination polyhedron of Sm^{3+} ions; (c) Coordination environments of Eu^{3+} ions with the H atoms omitted for clarity; symmetry codes: a = 1–x, –1+y, 1.5–z; b = 0.5–x, –0.5+y, 1.5–z; c = x, –y, 0.5+z; d = 1–x, 1–y, 2–z; e = x, 1–y, 0.5+z; (d) Coordination polyhedron of Eu^{3+} ions; (e) Coordination environments of Gd^{3+} ions with the H atoms omitted for clarity; symmetry codes: a = 0.5–x, 0.5+y, 2.5–z; b = 1+x, 2–y, 0.5+z; c = 1–x, 1+y, 2.5–z; d = 1–x, y, 2.5–z; e = 1+x, y, 1+z; (f) Coordination polyhedron of Gd^{3+} ions; (g) Coordination environments of Dy^{3+} ions with the H atoms omitted for clarity; symmetry codes: a = 0.5–x, 0.5–y, –z; b = 1–x, –y, –z; c = –0.5+x, 0.5+y, z; d = –0.5+x, –0.5–y, –0.5+z; e = 0.5–x, –0.5–y, –z; (h) Coordination polyhedron of Dy^{3+} ions; (i) Coordination environments of Er^{3+} ions with the H atoms omitted for clarity; symmetry codes: a = 1–x, –y, 2–z; b = –0.5+x, 0.5+y, z; c = x, 1+y, z; d = 1–x, 1+y, 2.5–z; (j) Coordination polyhedron of Er^{3+} ions; (k) Coordination environments of Yb^{3+} ions with the H atoms omitted for clarity; symmetry codes: a = x, y, 1+z; b =

1.5–x, –0.5–y, 3–z; c = 0.5+x, –0.5+y, 1+ z; d = 0.5+x, 0.5+y, 1+ z; e = 1.5–x, 0.5+y, 3.5–z; (l) Coordination polyhedron of Yb^{3+} ions.

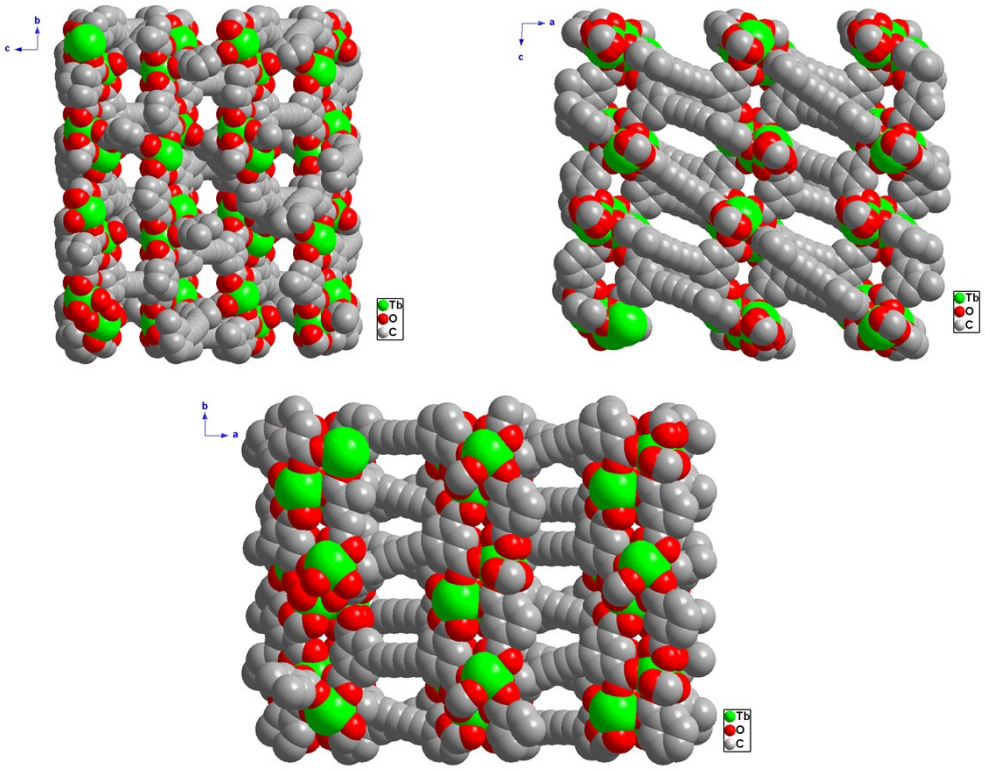

Fig. S7 Space filled representation of the 3–D framework in **4** seen from a, b, and c directions; Hydrogens, coordinated DMF molecules are omitted for clarity.

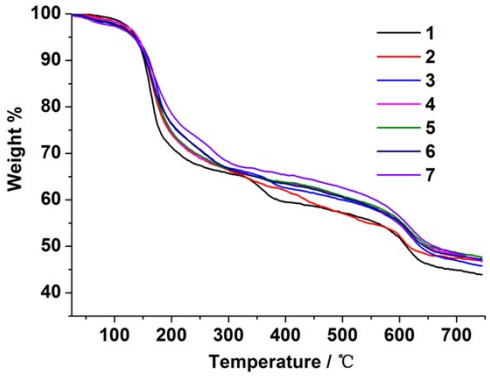

Fig. S8 The TG curves of **1–7**.

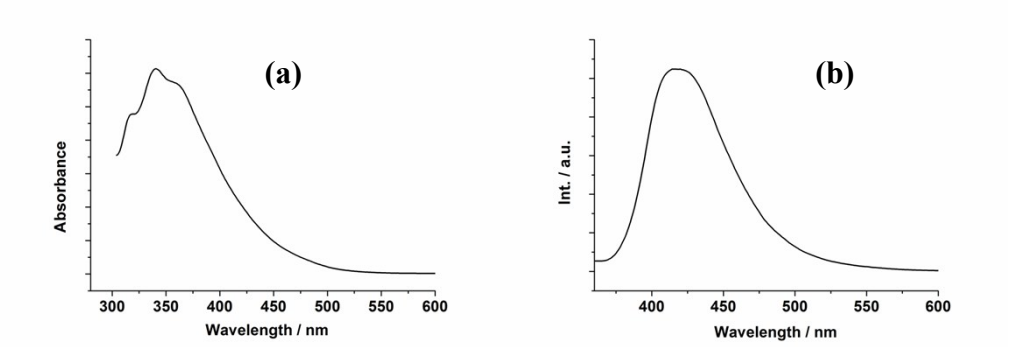

Fig. S9 (a) UV−vis absorption and (b) emission spectra of H_4BBTC in solid state at room temperature.

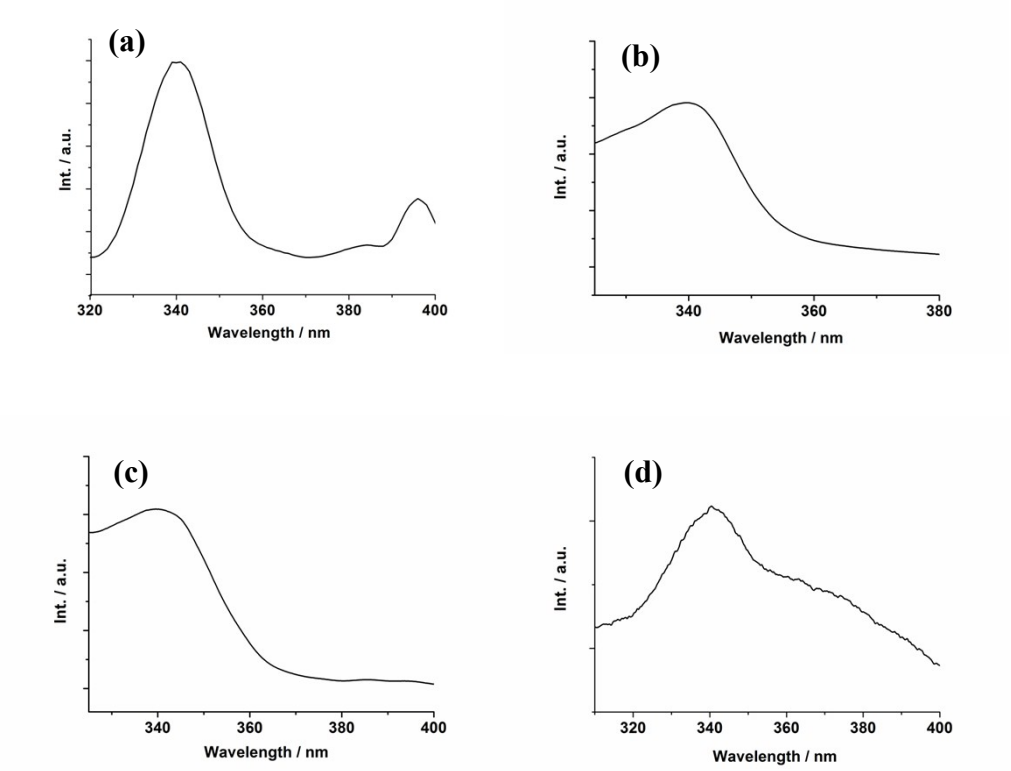

Fig. S10 The excitation spectra of **2** (a), **3** (b), **4** (c), and **5** (d) in solid state at room temperature, monitored at 615, 467, 542 and 576 nm, respectively.

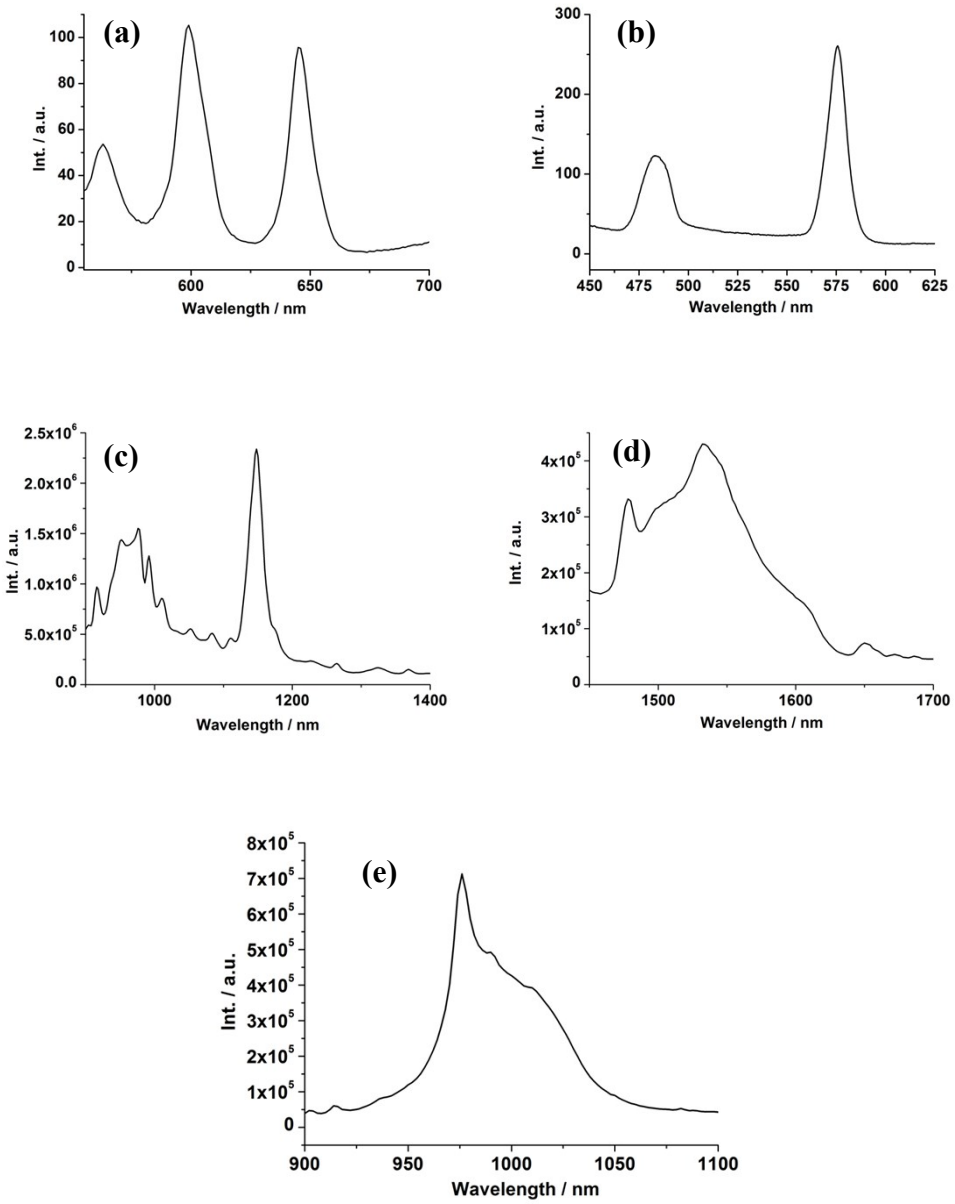

Fig. S11 Emission spectra of **1** (a) and **5** (b), and NIR emission spectra of **5** (c), **6** (d) and **7** (e).

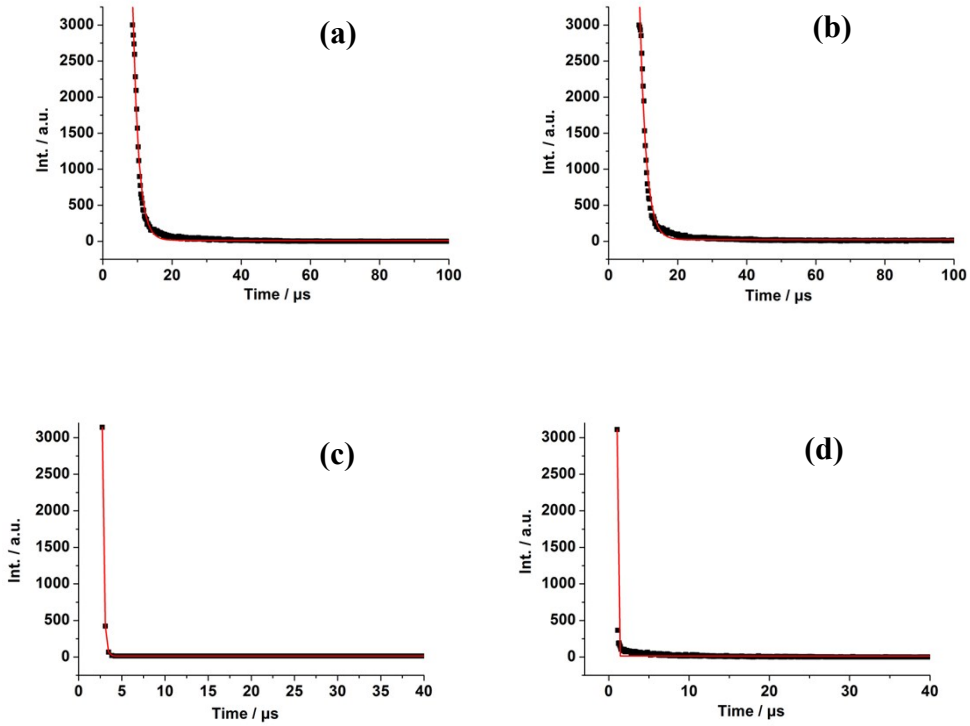

Fig. S12 Luminescence decay profiles for **1** (a), **5** (b), **6** (c) and **7** (d).

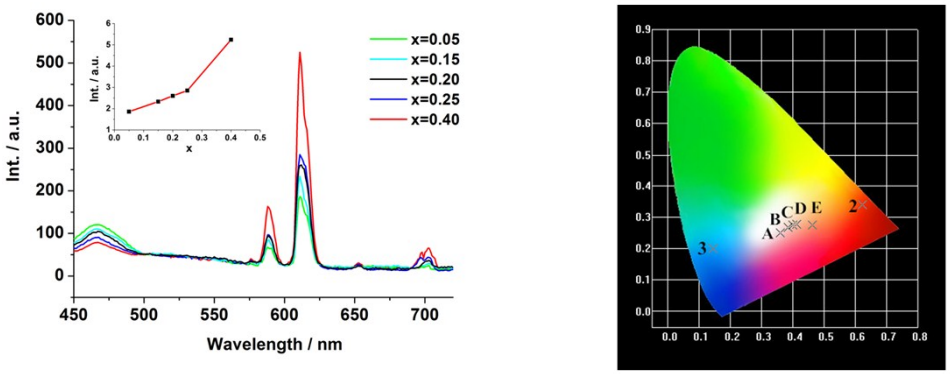

(a) **(b)**

Fig. S13 (a) Emission spectra of $\mathbf{Eu_xGd_{1-x}}$**−BBTC** with wide ranges of x = 0.05−0.4 (λ_{ex} = 340 nm) in the solid state at room temperature and plot of luminescence intensity of the band corresponding to the $^5D_0 \rightarrow {}^7F_2$ transition of Eu^{3+} ions against Eu^{3+} ions concentration; (b) CIE chromaticity diagram for $\mathbf{Eu_xGd_{1-x}}$**−BBTC** excited at 340 nm. $\mathbf{Eu_xGd_{1-x}}$**−BBTC** (Eu, Gd%): **3** (0, 100), **A** (5, 95), **B** (15, 85), **C** (20, 80), **D** (25, 75), **E** (40, 60) and **2** (100, 0).

Table S8 The corresponding CIE coordinates of the **Eu_xGd_{1-x}−BBTC** excited at 340nm

CIE chromaticity coordinates	
Gd−BBTC	(0.144, 0.199)
$Eu_{0.05}Gd_{0.95}$−BBTC	(0.360, 0.251)
$Eu_{0.15}Gd_{0.85}$−BBTC	(0.384, 0.267)
$Eu_{0.20}Gd_{0.80}$−BBTC	(0.400, 0.274)
$Eu_{0.25}Gd_{0.75}$−BBTC	(0.412, 0.277)
$Eu_{0.4}Gd_{0.6}$−BBTC	(0.463, 0.276)
Eu−BBTC	(0.622, 0.340)

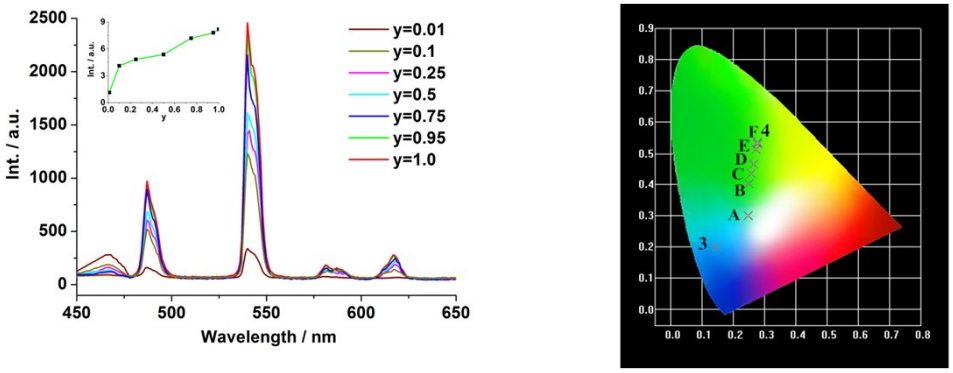

(a) **(b)**

Fig. S14 (a) Emission spectra of **Tb_yGd_{1-y}−BBTC** with the ranges of y = 0.01−1.0 (λ_{ex} = 340 nm) in the solid state at room temperature and Plot of luminescence intensity (the $^5D_4 \rightarrow {}^7F_5$ band) of Tb^{3+} ions against Tb^{3+} ion concentration; (b) CIE chromaticity diagram for **Tb_yGd_{1-y}−BBTC** excited at 340 nm. **Tb_yGd_{1-y}−BBTC** (Tb, Gd%): **3** (0, 100), **A** (1, 99), **B** (10, 90), **C** (25, 75), **D** (50, 50), **E** (75, 25), **F** (95, 5) and **4** (100, 0).

Table S9 The corresponding CIE coordinates of the $\mathbf{Tb_yGd_{1-y}}$**−BBTC** excited at 340 nm

CIE chromaticity coordinates	
$\mathbf{Tb_{0.01}Gd_{0.99}}$**−BBTC**	(0.247, 0.299)
$\mathbf{Tb_{0.1}Gd_{0.9}}$**−BBTC**	(0.251, 0.402)
$\mathbf{Tb_{0.25}Gd_{0.75}}$**−BBTC**	(0.258, 0.434)
$\mathbf{Tb_{0.5}Gd_{0.5}}$**−BBTC**	(0.265, 0.464)
$\mathbf{Tb_{0.75}Gd_{0.25}}$**−BBTC**	(0.273, 0.512)
$\mathbf{Tb_{0.95}Gd_{0.05}}$**−BBTC**	(0.277, 0.531)
Tb−BBTC	(0.278, 0.536)

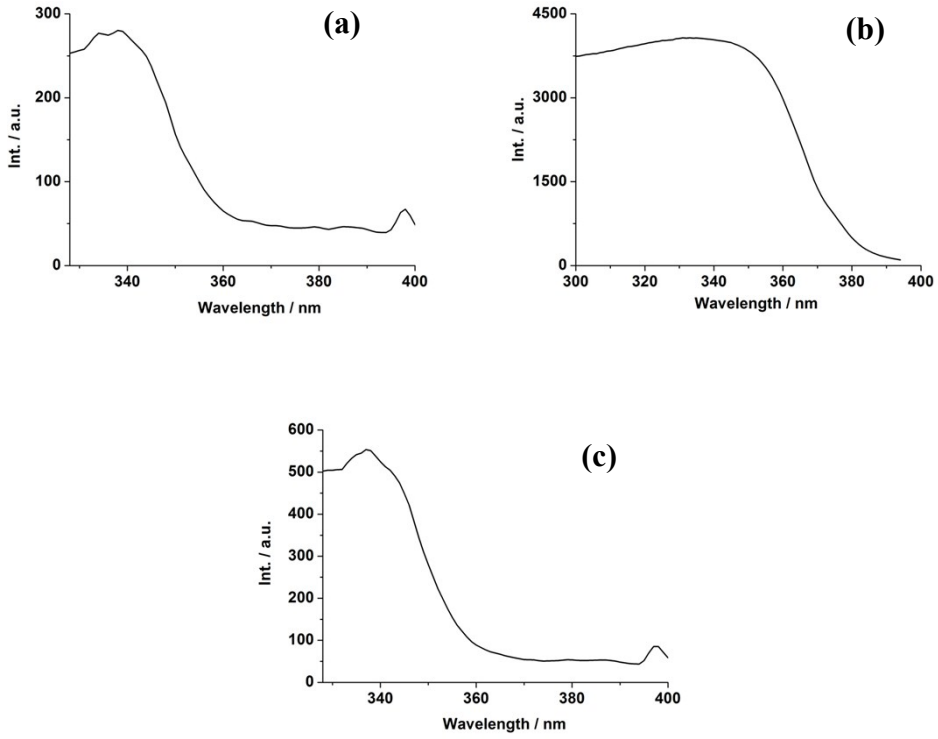

Fig. S15 The excitation spectra of $\mathbf{Eu_{0.25}Gd_{0.75}}$**−BBTC** (a), $\mathbf{Tb_{0.5}Gd_{0.5}}$**−BBTC** (b), and $\mathbf{Eu_{0.015}Tb_{0.035}Gd_{0.95}}$**−BBTC** (c) in solid state at room temperature, monitored at 615, 542 and 615 nm, respectively.

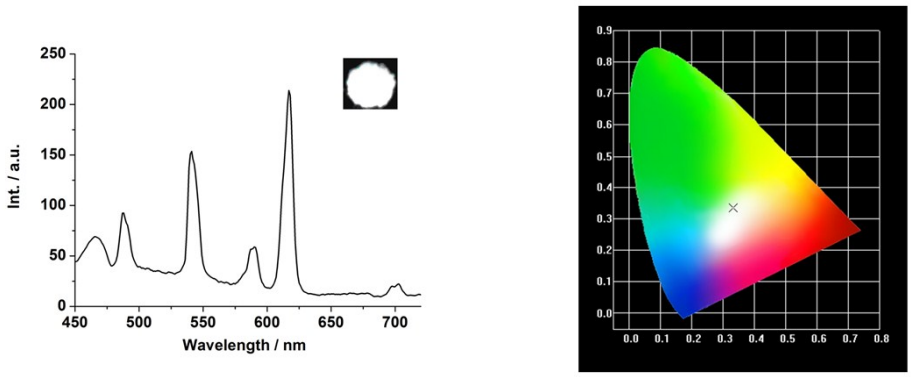

(a) **(b)**

Fig. S16 (a) Emission spectra and (b) CIE chromaticity diagram for **$Eu_{0.015}Tb_{0.035}Gd_{0.95}$−BBTC** excited at 340 nm.

Table S10 The corresponding CIE coordinates of the **$Eu_xTb_yGd_{1-x-y}$−BBTC** excited at 340nm

CIE chromaticity coordinates	
$Eu_{0.045}Tb_{0.055}Gd_{0.9}$−BBTC	(0.386, 0.409)
$Eu_{0.04}Tb_{0.05}Gd_{0.91}$−BBTC	(0.370, 0.403)
$Eu_{0.03}Tb_{0.045}Gd_{0.925}$−BBTC	(0.344, 0.391)
$Eu_{0.025}Tb_{0.04}Gd_{0.935}$−BBTC	(0.345, 0.364)
$Eu_{0.015}Tb_{0.035}Gd_{0.95}$−BBTC	**(0.334, 0.336)**

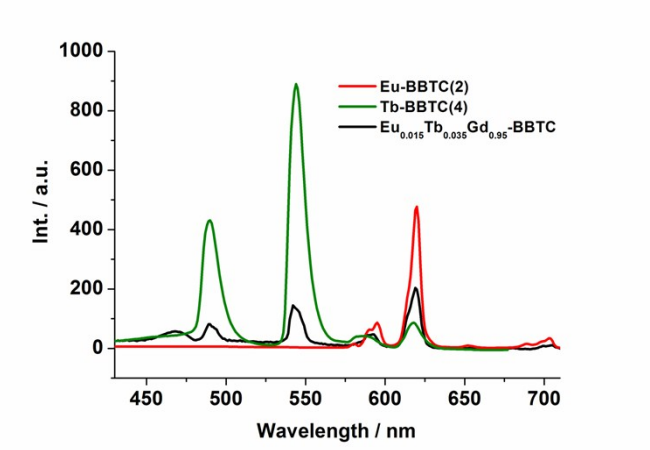

Fig. S17 Emission spectra of complexes **2**, **4** and the doped **$Eu_{0.015}Tb_{0.035}Gd_{0.95}$−BBTC** complex excited at 340 nm.

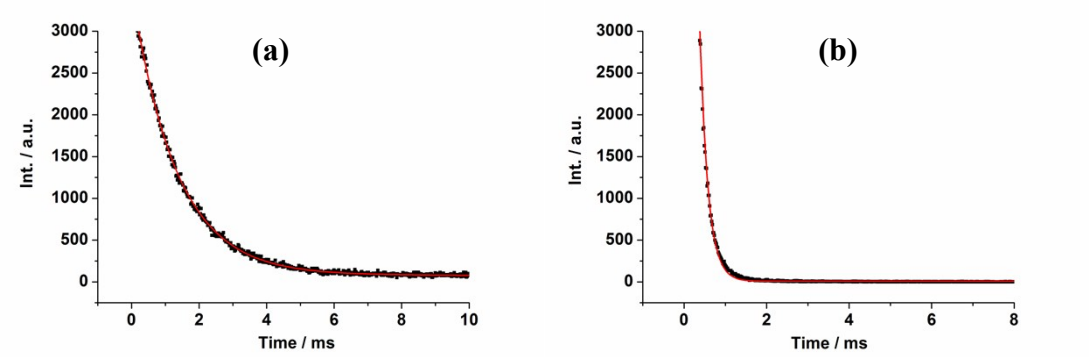

Fig. S18 Luminescence decay profiles of Eu^{3+} (a) and Tb^{3+} (b) in the doped complex **$Eu_{0.015}Tb_{0.035}Gd_{0.95}$−BBTC** excited at 340 nm (monitored at 615 nm for Eu^{3+} (a), and 542 nm for Tb^{3+} (b), respectively).